

# Investigation of double beta decay of $^{100}\text{Mo}$ to excited states of $^{100}\text{Ru}$

R. Arnold<sup>a</sup>, C. Augier<sup>b</sup>, A.S. Barabash<sup>c,\*</sup>, A. Basharina-Freshville<sup>d</sup>,  
 S. Blondel<sup>b</sup>, S. Blot<sup>e</sup>, M. Bongrand<sup>b</sup>, V. Brudanin<sup>f</sup>, J. Busto<sup>g</sup>,  
 A.J. Caffrey<sup>h</sup>, P. Čermák<sup>i</sup>, C. Cerna<sup>j</sup>, A. Chapon<sup>k</sup>, E. Chauveau<sup>e</sup>,  
 L. Dragounová<sup>l</sup>, D. Duchesneau<sup>m</sup>, D. Durand<sup>k</sup>, V. Egorov<sup>f</sup>, G. Eurin<sup>b,d</sup>,  
 J.J. Evans<sup>e</sup>, R. Flack<sup>d</sup>, X. Garrido<sup>b</sup>, H. Gómez<sup>b</sup>, B. Guillon<sup>k</sup>, P. Guzowski<sup>e</sup>,  
 R. Hodák<sup>i</sup>, P. Hubert<sup>j</sup>, C. Hugon<sup>j</sup>, J. Hůlka<sup>l</sup>, S. Jullian<sup>b</sup>, A. Klimenko<sup>f</sup>,  
 O. Kochetov<sup>f</sup>, S.I. Konovalov<sup>c</sup>, V. Kovalenko<sup>f</sup>, D. Lalanne<sup>b</sup>, K. Lang<sup>n</sup>,  
 Y. Lemièrè<sup>k</sup>, Z. Liptak<sup>n</sup>, P. Loaiza<sup>o</sup>, G. Lutter<sup>j</sup>, F. Mamedov<sup>i</sup>, C. Marquet<sup>j</sup>,  
 F. Mauger<sup>k</sup>, B. Morgan<sup>p</sup>, J. Mott<sup>d</sup>, I. Nemchenok<sup>f</sup>, M. Nomachi<sup>q</sup>, F. Nova<sup>n</sup>,  
 F. Nowacki<sup>a</sup>, H. Ohsumi<sup>r</sup>, R.B. Pahlka<sup>n</sup>, F. Perrot<sup>j</sup>, F. Piquemal<sup>j,o</sup>,  
 P. Povinec<sup>s</sup>, Y.A. Ramachers<sup>p</sup>, A. Remoto<sup>m</sup>, J.L. Reyss<sup>t</sup>, B. Richards<sup>d</sup>,  
 C.L. Riddle<sup>h</sup>, E. Rukhadze<sup>i</sup>, N. Rukhadze<sup>f</sup>, R. Saakyan<sup>d</sup>, X. Sarazin<sup>b</sup>,  
 Yu. Shitov<sup>u,f</sup>, L. Simard<sup>b,v</sup>, F. Šimkovic<sup>s</sup>, A. Smetana<sup>i</sup>, K. Smolek<sup>i</sup>,  
 A. Smolnikov<sup>f</sup>, S. Söldner-Rembold<sup>e</sup>, B. Souléj, I. Štekl<sup>i</sup>, J. Suhonen<sup>w</sup>,  
 C.S. Sutton<sup>x</sup>, G. Szklarz<sup>b</sup>, J. Thomas<sup>d</sup>, V. Timkin<sup>f</sup>, S. Torre<sup>d</sup>, V.I. Tretyak<sup>f</sup>,  
 V.I. Tretyak<sup>y</sup>, V. Umatov<sup>c</sup>, C. Vilela<sup>d</sup>, V. Vorobel<sup>z</sup>, G. Warot<sup>o</sup>, D.  
 Waters<sup>d</sup>, A. Žukauskas<sup>z</sup>

(The NEMO-3 Collaboration)

<sup>a</sup>IPHC, UPL, CNRS/IN2P3, F-67037 Strasbourg, France

<sup>b</sup>LAL, Univ Paris-Sud, CNRS/IN2P3, F-91405 Orsay, France

<sup>c</sup>ITEP, Institute of Theoretical and Experimental Physics, 117218 Moscow, Russia

<sup>d</sup>University College London, London WC1E 6BT, United Kingdom

<sup>e</sup>University of Manchester, Manchester M13 9PL, United Kingdom

<sup>f</sup>JINR, Joint Institute for Nuclear Research, 141980 Dubna, Russia

<sup>g</sup>CPPM, Université de Marseille, CNRS/IN2P3, F-13288 Marseille, France

<sup>h</sup>Idaho National Laboratory, Idaho Falls, ID 83415, U.S.A.

<sup>i</sup>IEAP, Czech Technical University in Prague, CZ-12800 Prague, Czech Republic

<sup>j</sup>CENBG, Université Bordeaux, CNRS/IN2P3, F-33175 Gradignan, France

<sup>k</sup>LPC Caen, ENSICAEN, Université de Caen, CNRS/IN2P3, F-14050 Caen, France

<sup>l</sup>National Radiation Protection Institute, CZ-14000 Prague, Czech Republic

<sup>m</sup>LAPP, Université de Savoie, CNRS/IN2P3, F-74941 Annecy-le-Vieux, France

<sup>n</sup>University of Texas at Austin, Austin, TX 78712, U.S.A.

---

\*Corresponding author

<sup>o</sup>Laboratoire Souterrain de Modane CNRS/CEA, F-73500 Modane, France  
<sup>p</sup>University of Warwick, Coventry CV4 7AL, United Kingdom  
<sup>q</sup>Osaka University, 1-1 Machikaney arna Toyonaka, Osaka 560-0043, Japan  
<sup>r</sup>Saga University, Saga 840-8502, Japan  
<sup>s</sup>FMFI, Comenius University, SK-842 48 Bratislava, Slovakia  
<sup>t</sup>LSCE, CNRS, F-91190 Gif-sur-Yvette, France  
<sup>u</sup>Imperial College London, London SW7 2AZ, United Kingdom  
<sup>v</sup>Institut Universitaire de France, F-75005 Paris, France  
<sup>w</sup>Jyväskylä University, FIN-40351 Jyväskylä, Finland  
<sup>x</sup>MHC, South Hadley, Massachusetts 01075, U.S.A.  
<sup>y</sup>Institute for Nuclear Research, MSP 03680, Kyiv, Ukraine  
<sup>z</sup>Charles University in Prague, Faculty of Mathematics and Physics, CZ-12116 Prague, Czech Republic

---

## Abstract

Double beta decay of  $^{100}\text{Mo}$  to the excited states of daughter nuclei has been studied using a  $600\text{ cm}^3$  low-background HPGe detector and an external source consisting of 2588 g of 97.5% enriched metallic  $^{100}\text{Mo}$ , which was formerly inside the NEMO-3 detector and used for the NEMO-3 measurements of  $^{100}\text{Mo}$ . The half-life for the two-neutrino double beta decay of  $^{100}\text{Mo}$  to the excited  $0_1^+$  state in  $^{100}\text{Ru}$  is measured to be  $T_{1/2} = [7.5 \pm 0.6(\text{stat}) \pm 0.6(\text{syst})] \cdot 10^{20}$  yr. For other  $(0\nu + 2\nu)$  transitions to the  $2_1^+$ ,  $2_2^+$ ,  $0_2^+$ ,  $2_3^+$  and  $0_3^+$  levels in  $^{100}\text{Ru}$ , limits are obtained at the level of  $\sim (0.25 - 1.1) \cdot 10^{22}$  yr.

*Keywords:* Double beta decay;  $^{100}\text{Mo}$ ; Excited states

---

## 1. Introduction

Experiments with solar, atmospheric, reactor and accelerator neutrinos have provided compelling evidence for the existence of neutrino oscillations driven by non zero neutrino masses and neutrino mixing [1, 2, 4, 3, 6, 5, 7, 8, 9, 10, 11, 12] (see also reviews [13, 14, 15]). The detection and study of neutrinoless double beta  $(0\nu\beta\beta)$  decay may clarify the following problems of neutrino physics (see discussions in [16, 17, 18, 19, 20, 21]): (i) neutrino nature: whether the neutrino is a Dirac or a Majorana particle, (ii) absolute neutrino mass scale, (iii) the type of neutrino mass hierarchy (normal,

inverted, or quasidegenerate), (iv) CP violation in the lepton sector (measurement of the Majorana CP-violating phases).

Double beta decay with the emission of two neutrinos ( $2\nu\beta\beta$ ) is an allowed process of second order in the Standard Model. The  $2\nu\beta\beta$  decays provide the possibility of an experimental determination of the nuclear matrix elements (NME) involved in the double beta decay processes. This leads to the development of theoretical schemes for NME calculations both in connection with the  $2\nu\beta\beta$  decays as well as the  $0\nu\beta\beta$  decays (see, for example, [22, 23, 24, 25, 26]). At present,  $2\nu\beta\beta$  decay to the ground state of the final daughter nucleus has been measured for eleven nuclei:  $^{48}\text{Ca}$ ,  $^{76}\text{Ge}$ ,  $^{82}\text{Se}$ ,  $^{96}\text{Zr}$ ,  $^{100}\text{Mo}$ ,  $^{116}\text{Cd}$ ,  $^{128}\text{Te}$ ,  $^{130}\text{Te}$ ,  $^{136}\text{Xe}$ ,  $^{150}\text{Nd}$  and  $^{238}\text{U}$  (a review of the results is given in Ref. [27], for  $^{136}\text{Xe}$  see recent results of EXO [28] and KamLAND-Zen [29]). In addition two neutrino double electron capture was detected in  $^{130}\text{Ba}$  [30, 31].

The  $\beta\beta$  decay can proceed through transitions to the ground state as well as to various excited states of the daughter nucleus. Studies of the latter transitions allow one to obtain supplementary information about  $\beta\beta$  decay. Because of the smaller transition energies, the probabilities for  $\beta\beta$  decay to excited states are substantially suppressed in comparison with transitions to the ground state, but as it was shown in Ref. [32], by using low-background High Purity Germanium (HPGe) detectors, the  $2\nu\beta\beta$  decay to the  $0_1^+$  level in the daughter nucleus may be detected for such nuclei as  $^{100}\text{Mo}$ ,  $^{96}\text{Zr}$ , and  $^{150}\text{Nd}$ . For these isotopes the energies involved in the  $\beta\beta$  transitions are large enough (1904, 2202, and 2631 keV, respectively), and the expected half-lives are of the order of  $10^{20} - 10^{21}$  yr. The double beta decay of  $^{100}\text{Mo}$  to the  $0^+$  excited state at 1130.3 keV of  $^{100}\text{Ru}$  was first observed in [33], and later confirmed in independent experiments [34, 35, 36, 37, 38, 39]. In 2004, the transition was detected in  $^{150}\text{Nd}$  for the first time [40, 41]. For  $^{96}\text{Zr}$  only a limit has been obtained up to now ( $T_{1/2} > 6.8 \cdot 10^{19}$  yr [42]). Additional isotopes ( $^{82}\text{Se}$ ,  $^{130}\text{Te}$ ,  $^{116}\text{Cd}$ , and  $^{76}\text{Ge}$ ) have also become of interest to studies of the  $2\nu\beta\beta$  decay to the  $0_1^+$  level (see reviews in Refs. [43, 44, 45]).

Recently it was speculated [46] that neutrinos may violate the Pauli exclusion principle (PEP) and therefore, at least partly obey Bose-Einstein statistics (see also [47]). As a consequence, neutrinos could form a Bose condensate which may account for parts or even all of the dark matter in the universe. As discussed in [48] the possible violation of the PEP has interesting consequences for  $2\nu\beta\beta$  decay. It not only modifies the energy and angular distributions of the emitted electrons, but it also strongly affects the  $2\nu\beta\beta$

decay rates to the ground and excited states in daughter nuclei. Following [48], the half-life ratios for transitions to excited  $2^+$  states and the  $0^+$  ground state are by far the most sensitive way of obtaining bounds on a substantial bosonic component to neutrino statistics. As a result, information on the decay rates to excited states is needed to test this new and potentially far-reaching hypothesis.

The  $0\nu\beta\beta$  transition to excited states of daughter nuclei provides a unique signature: in addition to two electrons with fixed total energy, one ( $0^+ \rightarrow 2_1^+$  transition) or two ( $0^+ \rightarrow 0_1^+$  transition) photons appear, with their energies being strictly fixed. In a hypothetical experiment detecting all decay products with a high efficiency and a high energy resolution, the background can be reduced to nearly zero. This zero background idea will be the goal of future experiments featuring a large mass of the  $\beta\beta$  sample (as mentioned in Refs. [43, 49, 50]). In Ref. [51] it was mentioned that detection of this transition will also give us the additional possibility of distinguishing between the various  $0\nu\beta\beta$  mechanisms (the light and heavy Majorana neutrino exchange mechanisms, the trilinear R-parity breaking mechanisms etc.).

In this article, results of an experimental investigation of the  $\beta\beta$  decay of  $^{100}\text{Mo}$  to the excited states of  $^{100}\text{Ru}$  are presented. The decay scheme for the triplet  $^{100}\text{Mo} - ^{100}\text{Tc} - ^{100}\text{Ru}$  [52] is shown in Fig. 1. The measurements have been carried out using a HPGe detector to look for  $\gamma$ -ray lines corresponding to the decay scheme. We study here transitions up to the 2051.7 keV level of  $^{100}\text{Ru}$ . Smaller phase space factors and thus smaller probabilities make it less useful to study the higher excited levels.

## 2. Experimental study

The experimental work was performed in the Modane Underground Laboratory (depth of 4800 m w.e.). A 600 cm<sup>3</sup> low-background HPGe detector was used to measure a 2588 g sample of enriched  $^{100}\text{Mo}$  metallic foil in a special delrin box which was placed around the detector endcap. This sample was formerly inside the NEMO-3 detector and used for the NEMO-3 measurements of  $^{100}\text{Mo}$  [53, 37]. Taking into account the concentration of Mo (99.8%) and enrichment (97.5%) there were 2518 g of  $^{100}\text{Mo}$  (or  $1.52 \cdot 10^{25}$  nuclei of  $^{100}\text{Mo}$ ) in the sample. Data were collected for 2288 h.

The Ge spectrometer is composed of a p-type crystal. The cryostat, endcap, and the other mechanical parts are made of a very pure Al-Si alloy. The

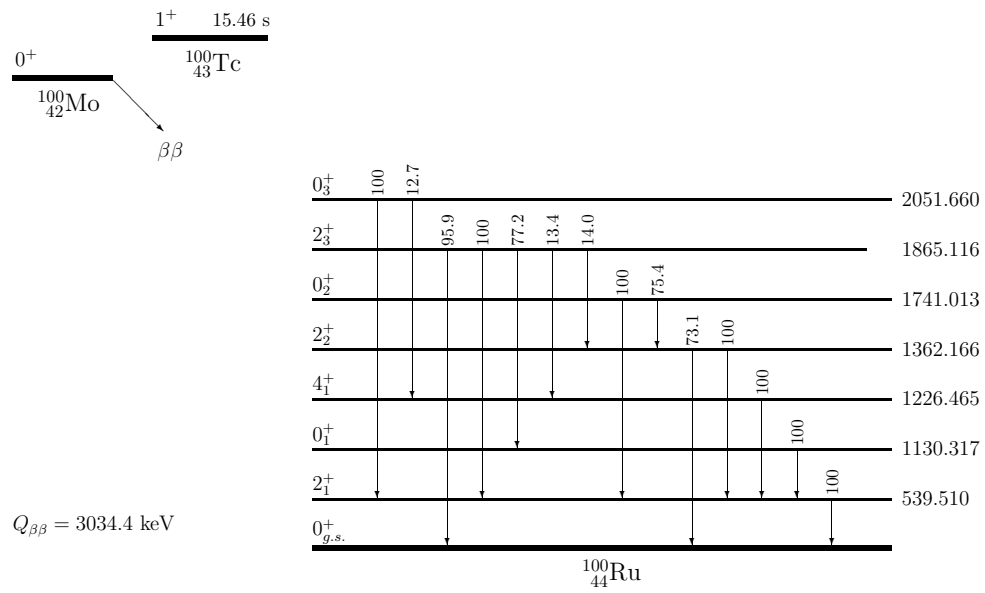


Figure 1: The decay scheme of  $^{100}\text{Mo}$ , taken from [52]. Only the investigated levels of  $0^+$  and  $2^+$  and  $4^+$  level associated with investigated transitions are shown. The relative main branching ratios from each level are presented.

cryostat has a U-type geometry to shield the crystal from radioactive impurities in the dewar. The passive shielding consists of three layers of Roman lead (which can be removed to host different sample volumes) with a total thickness of  $\sim 12$  cm and an external layer of  $\sim 20$  cm of low radioactivity lead. The activity of Roman lead is below 100 mBq/kg and the activity of low radioactivity lead is  $\sim 5$ -20 Bq/kg. To remove  $^{222}\text{Rn}$  gas, a special effort was made to minimize the free space near the detector and, in addition, the passive shielding is flushed with radon-depleted air (concentration of  $^{222}\text{Rn}$  is  $\sim 15$  mBq/m<sup>3</sup>) from a radon trapping facility.

The electronics consist of currently available spectrometric amplifiers and a 16384 channel ADC. The energy calibration is adjusted to cover the energy region from 5 keV to 3.5 MeV (the detector is sensitive to energies up to 6 MeV), and the energy resolution is 2.0 keV for the 1332-keV line of  $^{60}\text{Co}$ . The electronics are stable during the experiment due to the constant conditions in the laboratory (temperature of  $\approx 23^\circ$  C, hygrometric degree of  $\approx 50\%$ ).

All necessary information about radioactive isotopes was taken from databases of the National Nuclear Data Center [54] and were used for analysis of the energy spectrum. The photon detection efficiency for each investigated process has been calculated with the Monte Carlo (MC) code GEANT 3.21 [55] (and re-checked with GEANT 4 [56]).

To increase the accuracy of the efficiency calculations, special calibration measurements using radioactive sources with well-known activity ( $^{238}\text{U}$ ,  $^{152}\text{Eu}$  and  $^{138}\text{La}$ ) have been carried out.

The uranium source, with a diameter of 47 mm and height of 3 mm, contained 5.74 g of uranium ore (IAEA-RGU-1 reference material [57]) with an activity of  $(28.36 \pm 0.09)$  Bq. Two measurements were carried out: in the first case the source was placed directly on the endcap (in the center) of the HPGe detector, and in the second, it was shifted by 33 mm above the endcap. More than 10 different energy gamma-rays (from  $^{214}\text{Pb}$  and  $^{214}\text{Bi}$ ) in the region (100-2500) keV were used for the calibration.

The europium source was a point-like source with an activity  $(2323 \pm 46)$  Bq. The source was placed 310 mm above the endcap. More than 10 different energy gamma-rays in the region (122-1408) keV were used for the calibration.

In the case of the lanthanum, the source was a mixture of powdery filler (934 g of flour) and  $\text{La}_2\text{O}_3$  powder (238 g). This mix was moulded into approximately the same geometry and size as the box used in the  $^{100}\text{Mo}$  measurement. Taking into account the abundance of  $^{138}\text{La}$  ( $(0.0888 \pm 0.0007)$

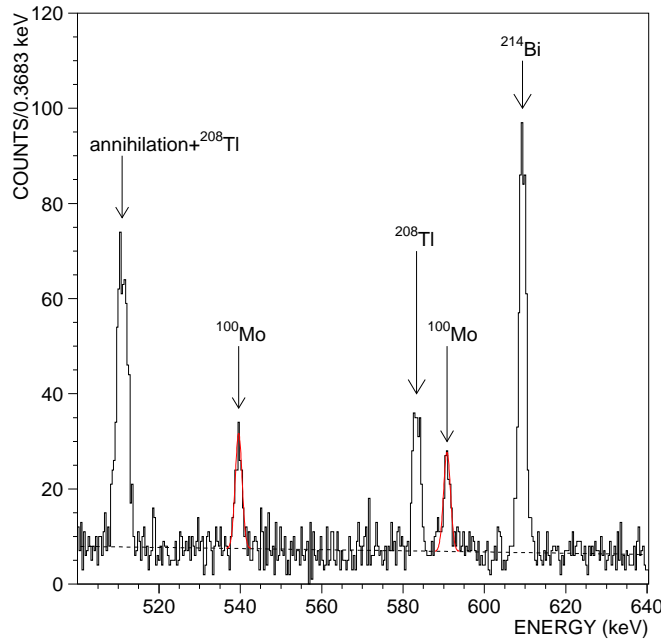


Figure 2: Energy spectrum from enriched Mo in the range [500-640] keV. The dashed line is the estimated continuous background and colored lines are the fitted peaks at 539.5 and 590.8 keV (see text).

% [58]) and its half-life ( $T_{1/2} = (1.02 \pm 0.01) \cdot 10^{11}$  yr [58]) it is possible to calculate precisely the activity of  $^{138}\text{La}$ :  $(168 \pm 2)$  Bq. Two gamma-rays are emitted with energies 788 and 1435 keV.

The results of these calibration measurements were used to check the accuracy of the MC simulations. The MC calculations for efficiency were adjusted to the results of the calibration measurements changing some parameters of the detector (mainly by increasing the dead layer of the HPGe detector). As a result discrepancies between experimental and simulated efficiencies do not exceed 7% for all gamma lines of the 3 sources.

Figures 2, 3, and 4 show the energy spectra in the ranges of interest. Arrows indicate the position of the peaks under study.

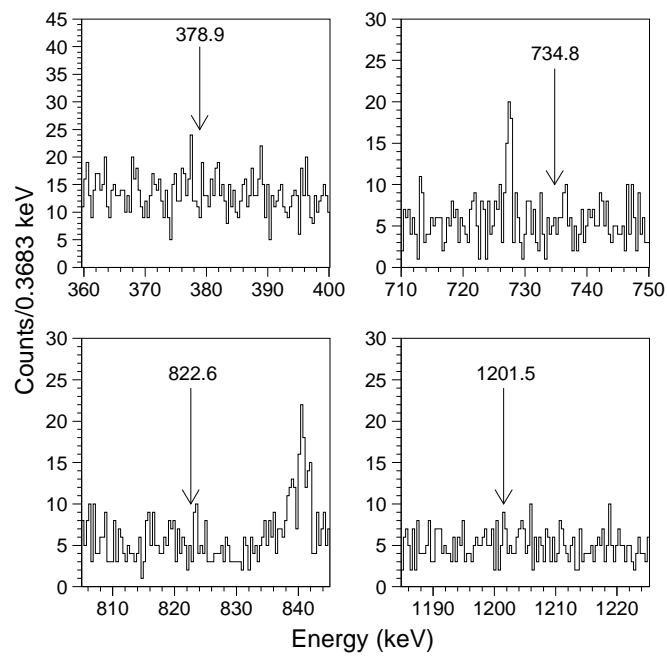


Figure 3: Energy spectrum from enriched Mo in the range [360-400], [710-750], [800-850] and [1180-1230] keV.



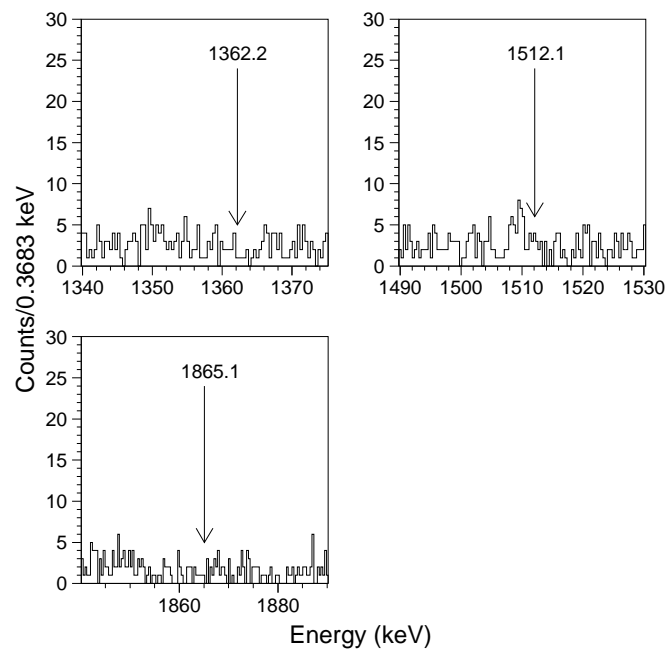


Figure 4: Energy spectrum from enriched Mo in the ranges [1340-1380], [1490-1530] and [1840-1890] keV.

### 3. Analysis and results

#### 3.1. Decay to the $0_1^+$ excited state

This transition is accompanied by two  $\gamma$ -rays with energies of 539.5 keV and 590.8 keV (see Fig. 1). The detection photopeak efficiencies are equal to 3.29% at 539.5 keV and 3.22% at 590.8 keV. These values were obtained using MC simulations. The calculation included the effects of the extended geometry, the attenuation of the  $\gamma$ -rays in the sample, the full-energy peak efficiency of the germanium detector, the summing effects in the detector and the anisotropic angular correlation between the  $\gamma$ -rays emitted after  $2\beta$  decay of  $^{100}\text{Mo}$  to the  $0_1^+$  excited state of  $^{100}\text{Ru}$ . Fig. 2 shows the energy spectrum in the range of interest. Both peaks at 539.5 keV and 590.8 keV are clearly visible. In addition there are also peaks from background at 511 keV (annihilation +  $^{208}\text{Tl}$ ), 583.2 keV ( $^{208}\text{Tl}$ ) and 609.3 keV ( $^{214}\text{Bi}$ ). The averaged continuous background (dashed line) is obtained by fitting a parabola to the (500-640) keV energy range after removing counts under peaks around 511, 539.5, 583.2, 590.8 and 609.3 keV. Then the peaks at 539.5 and 590.8 keV are fitted by Gaussians with energy resolution equal to 2.0 keV (colored lines). The average energy resolution over the entire period of measurements was established by fitting the neighboring 609 keV  $\gamma$ -line,  $(2.0 \pm 0.1)$  keV. Finally, the peak at 539.5 keV is at  $129 \pm 14$  counts, and the peak at 590.8 keV is at  $110 \pm 13$  counts. It corresponds to  $T_{1/2} = 7.0_{-0.7}^{+0.9}(\text{stat}) \cdot 10^{20}$  yr for the 539.5 keV peak and  $T_{1/2} = 8.0_{-0.8}^{+1.1}(\text{stat}) \cdot 10^{20}$  yr for 590.8 keV peak. Summing the two peaks we obtain a signal of  $239 \pm 19$  events, corresponding to a half-life of  $^{100}\text{Mo}$  to the first  $0^+$  excited state of  $^{100}\text{Ru}$  given by  $T_{1/2} = [7.5 \pm 0.6(\text{stat}) \pm 0.6(\text{syst})] \cdot 10^{20}$  yr. The primary systematic comes from the efficiency calculations (7%), the estimation of the number of useful events (4%) and the uncertainties in the geometrical position of the  $^{100}\text{Mo}$  sample (2%). The uncertainty in the number of useful events is connected with an error in the definition of the average background in the region of the studied peaks and the choice of the fitting procedure. The uncertainty connected with the inaccuracy in the position of the  $^{100}\text{Mo}$  sample in relation to the position of the crystal was estimated by the MC, changing the position of the sample by  $\pm 3$  mm along a crystal axis and changing the external diameter of the sample by  $\pm 4$  mm.

### 3.2. Decay to the $2_1^+$ excited state

To search for this transition, one has to look for a gamma-ray with an energy of 539.5 keV. For this single gamma-ray, the detection efficiency is 4.02%. Decays to the  $0_1^+$  state also contribute to a peak at this energy. In the analysis given above, two measurements of the half life for decays to the  $0_1^+$  state are given, obtained independently from the 539.5 keV and 590.8 keV peaks. These two measurements are consistent with each other. Since the 590.8 keV peak contains only photons from decays to the  $0_1^+$  state, this shows that the observed peak at 539.8 keV is consistent with decays to only the  $0_1^+$  state. Therefore, one can only give a lower limit on the half life for transitions to the  $2_1^+$  excited state of  $^{100}\text{Ru}$ . The contribution to the 539.5 keV peak from  $2\nu$  decay to the  $0_1^+$  excited state was estimated as  $112 \pm 13$  events (using the observed number of events in 590.8 keV peak and taking into account the difference in the efficiency). The excess of  $17 \pm 19$  counts indicates that there is no signal. The 90% C.L. upper limit on the number of observed events for the decay to the  $2_1^+$  state is  $43.5^1$ , yielding a limit on the half life of  $T_{1/2} > 2.5 \cdot 10^{21}$  yr. The limits obtained from other measurements, together with available data on  $\beta\beta$  decay of  $^{100}\text{Mo}$  are presented in Table 1.

### 3.3. Decays to the $2_2^+$ , $2_3^+$ , $0_2^+$ and $0_3^+$ excited states

To search for these transitions one has to look for  $\gamma$ -rays with energies of 378.9, 734.8, 822.6, 1201.5, 1362.2, 1512.1 and 1865.1 keV (Fig. 1). As one can see from figures 3 and 4, there are no statistically significant peaks at these energies.

The Bayesian approach [59] has been used to estimate limits. To construct the likelihood function, every bin of the spectrum is assumed to have a Poisson distribution with its mean  $\mu_i$  and the number of events equal to the content of the  $i$ th bin. The mean can be written in the general form,

$$\mu_i = N \sum_m \varepsilon_m a_{mi} + \sum_k P_k a_{ki} + b_i. \quad (1)$$

The first term in (1) describes the contribution of the investigated process that may have a few  $\gamma$ -lines contributing appreciably to the  $i$ th bin. The parameter  $N$  is the number of decays,  $\varepsilon_m$  is the detection efficiency of the

---

<sup>1</sup>This value is obtained by integrating the Gaussian function (with mean value 17 and sigma 19) from 0 to 43.5 to obtain 90% probability.

Table 1: Experimental results for  $(0\nu + 2\nu)\beta\beta$  decay of  $^{100}\text{Mo}$  to the excited states of  $^{100}\text{Ru}$ . Energy is presented in keV. All limits are given at the 90% C.L. <sup>a)</sup>Only  $0\nu$  decay mode. <sup>b)</sup>Half-life value for  $2\nu$  decay (see text for the details).

Excited state	Energy of $\gamma$ -rays (efficiency)	$(T_{1/2}^{0\nu+2\nu})_{exp}$ ( $10^{20}$ yr)	
		this work	other results
$2_1^+(539.5)$	539.5 (4.02%)	$> 25$	$> 16$ [33] $> 1600^a)$ [37]
$0_1^+(1130.3)$	539.5 (3.29%) 590.8 (3.22%)	$7.5 \pm 0.6(stat) \pm 0.6(syst)^b)$	see Table 2 $> 890^a)$ [37]
$2_2^+(1362.2)$	822.6 (1.72%) 1362.2 (1.34%)	$> 108$	$> 44$ [38]
$0_2^+(1741.0)$	378.9 (1.39%) 1201.5 (1.53%)	$> 40$	$> 48$ [38]
$2_3^+(1865.1)$	734.8 (0.65%) 1865.1 (0.85%)	$> 49$	$> 43$ [38]
$0_3^+(2051.7)$	1512.1 (2.09%)	$> 43$	$> 40$ [38]

$m$ th  $\gamma$ -line and  $a_{mi}$  is the contribution of the  $m$ th line to the  $i$ th bin. For low-background measurements, a  $\gamma$ -line may be taken to have a gaussian shape. The second term gives contributions of background  $\gamma$ -lines. Here  $P_k$  is the area of the  $k$ th  $\gamma$ -line and  $a_{ki}$  is its contribution to the  $i$ th bin. The third term represents the so-called ‘‘continuous background’’ ( $b_i$ ), which has been selected as a straight-line fit after rejecting all peaks in the region-of-interest. We select this region as the peak to be investigated  $\pm 30$  standard deviations ( $\approx 20$  keV). The likelihood function is the product of probabilities for selected bins. Normalizing over the parameter  $N$  gives the probability density function for  $N$ , which is used to calculate limits for  $N$ . To take into account errors in the  $\gamma$ -line shape parameters, peak areas, and other factors, one should multiply the likelihood function by the error probability distributions for these values and integrate, to provide the average probability density function for  $N$ .

The photon detection efficiency for each investigated process is computed using MC simulations. Finally the lower half-life limits are found in the range  $(0.4 - 1.1) \cdot 10^{22}$  yr for the transitions (Table 1). Table 1 also presents other limits on these transitions.

Table 2: Present “positive” results on  $2\nu\beta\beta$  decay of  $^{100}\text{Mo}$  to the first  $0^+$  excited state of  $^{100}\text{Ru}$ .  $N$  is the number of useful events,  $S/B$  is the signal-to-background ratio. <sup>a)</sup> Sum of two peaks. <sup>b)</sup> Sample was located between two HPGe detectors working in coincidence. <sup>c)</sup> The result was obtained using sum spectrum from 4 HPGe detectors. Using coincidence regime half-life was measured too, but with a few times worse accuracy.

$T_{1/2}$ , yr	$N$	$S/B$	Year, Ref.	Method
$6.1_{-1.1}^{+1.8}(\text{stat}) \times 10^{20}$	133 <sup>a)</sup>	$\sim 1/7$	1995 [33]	HPGe
$9.3_{-1.7}^{+2.8}(\text{stat}) \pm 1.4(\text{syst}) \times 10^{20}$	153 <sup>a)</sup>	$\sim 1/4$	1999 [34]	HPGe
$6.0_{-1.1}^{+1.9}(\text{stat}) \pm 0.6(\text{syst}) \times 10^{20}$	19.5	8/1	2001 [35, 36]	2xHPGe <sup>b)</sup>
$5.7_{-0.9}^{+1.3}(\text{stat}) \pm 0.8(\text{syst}) \times 10^{20}$	37.5	3/1	2007 [37]	NEMO-3
$5.5_{-0.8}^{+1.2}(\text{stat}) \pm 0.3(\text{syst}) \times 10^{20}$	35.5	8/1	2009 [38]	2xHPGe <sup>b)</sup>
$6.9_{-0.8}^{+1.0}(\text{stat}) \pm 0.7(\text{syst}) \times 10^{20}$	597 <sup>a)</sup>	1/10	2010 [39]	4xHPGe <sup>c)</sup>
$7.5 \pm 0.6(\text{stat}) \pm 0.6(\text{syst}) \times 10^{20}$	239 <sup>a)</sup>	2/1	2013, this work	HPGe

#### 4. Discussion

Because the technique used in the present work does not allow for a distinction between  $0\nu\beta\beta$  and  $2\nu\beta\beta$  decay, our result for double beta decay of  $^{100}\text{Mo}$  to the excited  $0_1^+$  state in  $^{100}\text{Ru}$  is the sum of the  $0\nu\beta\beta$  and  $2\nu\beta\beta$  processes. However the detection of only the  $2\nu\beta\beta$  decay is supported by the following argument - in the recent NEMO-3 paper [37] the limit on  $0\nu\beta\beta$  decay of  $^{100}\text{Mo}$  to the excited  $0_1^+$  state was established as  $8.9 \cdot 10^{22}$  yr, which is two orders of magnitude stronger than the half-life value obtained here. Therefore, it is safe to assume that our result for  $T_{1/2}$  refers solely to the  $2\nu\beta\beta$  decay. For the transition to the  $0_1^+$  excited state of  $^{100}\text{Ru}$  the obtained value is in a good agreement with results of previous experiments (see Table 2). Our result yields the best statistical accuracy, and one of the smallest systematic errors, of all previous measurements. As a result the most precise half-life value for  $2\nu$  transition of  $^{100}\text{Mo}$  to the  $0_1^+$  excited state of  $^{100}\text{Ru}$  is obtained.

Using the phase space factor value  $G = 6.055 \cdot 10^{-20} \text{ yr}^{-1}$  [60],  $g_A = 1.2701$  [61] and the measured half-life  $T_{1/2} = [7.5 \pm 0.6(\text{stat}) \pm 0.6(\text{syst})] \cdot 10^{20} \text{ yr}$ , we obtain a NME value for the  $2\nu\beta\beta$  transition to the  $0_1^+$  excited state of  $M_{2\nu}(0_1^+) = 0.092 \pm 0.006$  (scaled by the electron rest mass).<sup>2</sup> We can compare this value

<sup>2</sup>We use here the following relation,  $T_{1/2}^{-1} = g_A^4 \cdot G \cdot M_{2\nu}^2$ .  $T_{1/2}$  is the half-life value [yr],

with the NME value for the  $2\nu\beta\beta$  transition to the ground state of  $^{100}\text{Ru}$ ,  $M_{2\nu}(0_{g.s.}^+) = 0.1273_{-0.0034}^{+0.0038}$  (here we used the average half-life value  $T_{1/2} = (7.1 \pm 0.4) \cdot 10^{18}$  yr from [27],  $G = 3.308 \cdot 10^{-18}$  yr $^{-1}$  from [60] and  $g_A = 1.2701$  from [61]). Using  $G$  values obtained in the framework of the SSD (Single State Dominance) mechanism [60] we can obtain NME values for the transition to the  $0_1^+$  excited state and ground state of  $0.089 \pm 0.006$  and  $0.1139_{-0.0031}^{+0.0034}$  respectively. Independent of the NME model chosen,  $M_{2\nu}(0_{g.s.}^+)$  is  $\sim 25\%$  greater than  $M_{2\nu}(0_1^+)$  with a significance of more than  $4\sigma$ . The knowledge of these NMEs can be exploited for the deeper understanding of the underlying nuclear structure, i.e. for the development of more reliable nuclear structure models. We note that ratio of the half-lives and the corresponding ratio of NMEs is independent of the value of the axial-vector coupling constant  $g_A$ .

The observation of double beta decay to the  $2_1^+$  excited state is rather difficult above the background of the decay going to the  $0_1^+$  level. The experimental effect from the  $2_1^+$  decay is an additional contribution to the peak at an energy of 539.5 keV. In our case there is no significant excess. Therefore only a limit can be set,  $T_{1/2} > 2.5 \cdot 10^{21}$  yr. This limit can be compared with previous results,  $> 1.6 \cdot 10^{21}$  yr [33] and  $> 1.1 \cdot 10^{21}$  yr [37]. From the general point of view, the decay to the  $2^+$  excited state should be suppressed [62, 63]. Theoretical values for the half-life of this two neutrino transition usually lay in the interval  $\sim 10^{23} - 10^{26}$  yr [64, 65, 66, 67]. Nevertheless in Ref. [68] a more “optimistic” value ( $2.1 \cdot 10^{21}$  yr) was obtained which is however lower than the obtained experimental limit ( $2.5 \cdot 10^{21}$  yr). In the framework of the SSD mechanism, the prediction for this transition is  $\sim (1 - 3) \cdot 10^{23}$  yr [69, 70] which is quite far from the achieved sensitivity. In the scheme with a “bosonic” neutrino, the decay rate can be increased by  $\sim 100$  times [44]. It is therefore interesting and important to increase the sensitivity of such measurements.

For the double beta decay of  $^{100}\text{Mo}$  to the  $2_1^+$ ,  $2_2^+$ ,  $2_3^+$  and  $0_3^+$  excited states of  $^{100}\text{Ru}$  the obtained limits are better than the best previous results [38] (see Table 1).

---

$G$  is the phase space factor [yr $^{-1}$ ],  $g_A$  is the axial vector coupling constant and  $M_{2\nu}$  is the dimensionless nuclear matrix element.

## 5. Conclusion

Double beta decay of  $^{100}\text{Mo}$  to the excited states of daughter nuclei was investigated with a high level of sensitivity. The half-life for the  $2\nu\beta\beta$  decay of  $^{100}\text{Mo}$  to the excited  $0_1^+$  state in  $^{100}\text{Ru}$  is measured to be  $T_{1/2} = [7.5 \pm 0.6(\text{stat}) \pm 0.6(\text{syst})] \cdot 10^{20}$  yr. This is the most precise value yet obtained for this transition. For other  $(0\nu + 2\nu)$  transitions to the  $2_1^+$ ,  $2_2^+$ ,  $0_2^+$ ,  $2_3^+$  and  $0_3^+$  levels in  $^{100}\text{Ru}$ , the obtained limits are in the range of  $(0.25 - 1.1) \cdot 10^{22}$  yr. The limits for transitions to the  $2_1^+$ ,  $2_2^+$ ,  $2_3^+$  and  $0_3^+$  excited states are stronger than the previous results.

## Acknowledgements

The authors would like to thank the Modane Underground Laboratory staff for their technical assistance in running the experiment. Portions of this work were supported by grants from RFBR (no 12-02-12112 and 13-02-93107) and by grants LG11030 and LM2011027 (MEYS, Czech Republic).

## References

- [1] B.T. Cleveland et al., *Astrophys. J.* 496 (1998) 505.
- [2] Y. Fukuda et al., *Phys. Rev. Lett.* 77 (1996) 1683.
- [3] J.N. Abdurashitov et al., *Phys. Rev. C* 80 (2009) 015807.
- [4] P. Anselmann et al., *Phys. Lett. B* 285 (1992) 376; W. Hampel et al., *Phys. Lett. B* 447 (1999) 127; M. Altmann et al., *Phys. Lett. B* 616 (2005) 174.
- [5] S. Fukuda et al., *Phys. Lett. B* 539 (2002) 179.
- [6] Q.R. Ahmad et al., *Phys. Rev. Lett.* 87 (2001) 071301; 89 (2002) 011301.
- [7] Y. Fukuda et al., *Phys. Rev. Lett.* 81 (1998) 1562.
- [8] Y. Ashie et al., *Phys. Rev. Lett.* 93 (2004) 101801.
- [9] K. Eguchi et al., *Phys. Rev. Lett.* 90 (2003) 021802; T. Araki et al., *Phys. Rev. Lett.* 94 (2005) 081801.

- [10] C. Arpesella et al., Phys. Lett. B 658 (2008) 101; Phys. Rev. Lett. 101 (2008) 091302.
- [11] M.H. Ahn et al., Phys. Rev. D 74 (2006) 072003.
- [12] D.G. Michael et al., Phys. Rev. Lett. 97 (2006) 191801; P. Adamson et al., Phys. Rev. Lett. 101 (2008) 131802.
- [13] R.N. Mohapatra and A.Y. Smirnov, Annu. Rev. Nucl. Part. Sci. 56 (2006) 569.
- [14] S.M. Bilenky, Phys. Part. Nucl. 42 (2011) 515.
- [15] D.V. Forero, M. Tortola, and J.W.F. Valle, Phys. Rev. D 86 (2012) 073012.
- [16] R.N. Mohapatra et al., Rep. Prog. Phys. 70 (2007) 1757.
- [17] S. Pascoli, S.T. Petcov, and T. Schwetz, Nucl. Phys. B 734 (2006) 24.
- [18] J.D. Vergados, H. Ejiri, and F. Simkovic, Rep. Prog. Phys. 75 (2012) 106301.
- [19] S.M. Bilenky and C. Giunti, Mod. Phys. Let. A 27 (2012) 1230015.
- [20] W. Rodejohann, J. Phys. G 39 (2012) 124008.
- [21] F. Simkovic, S.M. Bilenky, A. Faessler, and Th. Gutsche, Phys. Rev. D 87 (2013) 073002.
- [22] V. Rodin, A. Faessler, F. Simkovic, and P. Vogel, Nucl. Phys. A 766 (2006) 107; 793 (2007) 213.
- [23] M. Kortelainen and J. Suhonen, Phys. Rev. C 75 (2007) 051303.
- [24] M. Kortelainen and J. Suhonen, Phys. Rev. C 76 (2007) 024315.
- [25] F. Simkovic et al., Phys. Rev. C 77 (2008) 045503.
- [26] J. Barea, J. Kotila, and F. Iachello, Phys. Rev. C 87 (2013) 014315.
- [27] A.S. Barabash, Phys. Rev. C 81 (2010) 035501.
- [28] M. Auger et al., Phys. Rev. Lett. 109 (2012) 032505.



- [29] A. Gando et al., Phys. Rev. C 85 (2012) 045504.
- [30] A.P. Meshik, C.M. Hohenberg, O.V. Pravdivtseva, and Ya.S. Kapusta, Phys. Rev. C 64 (2001) 035205.
- [31] M. Pujol, B. Marty, P. Burnard, and P. Philippot, Geochim. Cosmochim. Acta 73 (2009) 6834.
- [32] A.S. Barabash, JETP Lett. 51 (1990) 207; preprint ITEP 188-89 (1989).
- [33] A.S. Barabash et al., Phys. Lett. B 345 (1995) 408.
- [34] A.S. Barabash, R. Gurriaran, F. Hubert, Ph. Hubert, and V.I. Umatov, Phys. At. Nucl. 62 (1999) 2039.
- [35] L. De Braekeleer, M. Hornish, A. Barabash, and V. Umatov, Phys. Rev. Lett. 86 (2001) 3510.
- [36] M.J. Hornish, L. De Braekeleer, A.S. Barabash, and V.I. Umatov, Phys. Rev. C 74 (2006) 044314.
- [37] R. Arnold et al., Nucl. Phys. A 781 (2007) 209.
- [38] M.F. Kidd et al., Nucl. Phys. A 821 (2009) 251.
- [39] P. Belli et al., Nucl. Phys. A 846 (2010) 143.
- [40] A.S. Barabash, F. Hubert, Ph. Hubert, and V.I. Umatov, JETP Lett. 79 (2004) 10.
- [41] A.S. Barabash et al., Phys. Rev. C 79 (2009) 045501.
- [42] A.S. Barabash et al., J. Phys. G 22 (1996) 487.
- [43] A.S. Barabash, Czech. J. Phys. 50 (2000) 447.
- [44] A.S. Barabash, AIP Conf. Proc. 942 (2007) 8.
- [45] A.S. Barabash, Phys. At. Nucl. 73 (2010) 162.
- [46] A.D. Dolgov and A.Yu. Smirnov, Phys. Lett. B 621 (2005) 1.
- [47] L. Cucurull, J.A. Grifols, and R. Toldra, Astropart. Phys. 4 (1996) 391.

- [48] A.S. Barabash, A.D. Dolgov, R. Dvornicky, F. Simkovic, and A.Yu. Smirnov, Nucl. Phys. B 783 (2007) 90.
- [49] A.S. Barabash, Phys. At. Nucl. 67 (2004) 438.
- [50] J. Suhonen, Phys. Rev. C 62 (2000) 042501.
- [51] F. Simkovic and A. Faessler, Prog. Part. Nucl. Phys. 48 (2002) 201.
- [52] B. Singh, Nuclear Data Sheets 109 (2008) 297.
- [53] R. Arnold et al., Phys. Rev. Lett. 95 (2005) 182302.
- [54] <http://www.nndc.bnl.gov>
- [55] CERN Detector Description and Simulation Tool, CERN Program Library Long Writeup W5013 ([http://wwwasdoc.web.cern.ch/wwwasdoc/geant\\_html3/geantall.html](http://wwwasdoc.web.cern.ch/wwwasdoc/geant_html3/geantall.html)), 1995.
- [56] S. Agostinelli et al. (GEANT Collaboration), Nucl. Instr. Meth. A 506 (2003) 250 (<http://geant4.cern.ch>).
- [57] <http://nucleus.iaea.org/rpst/ReferenceProducts/ReferenceMaterials/Radionuclides/IAEA-RGU-1.htm>
- [58] A.A. Sonzogni, Nuclear Data Sheets 98 (2003) 515.
- [59] S. Eidelman *et al.*, Phys. Lett. B **592**, 1 (2004).
- [60] J. Kotila and F. Iachello, Phys. Rev. C 85 (2012) 034316.
- [61] J. Beringer et al. (Particle Data Group), Phys. Rev. D 86 (2012) 010001 (p. 1266).
- [62] W.C. Haxton and G.J. Stephenson, Prog. Part. Nucl. Phys. 12 (1984) 404.
- [63] M. Doi, T. Kotani, and E. Takasugi, Prog. Theor. Phys. Suppl. 83 (1985) 1.
- [64] J.G. Hirsch, O. Castanos, P.O. Hess, and O. Civitarese, Phys. Rev. C 51 (1995) 2252.

- [65] S. Stoica and I. Mihut, Nucl. Phys. A 602 (1996) 197.
- [66] J. Toivanen and J. Suhonen, Phys. Rev. C 55 2314 (1997).
- [67] C.M. Raduta and A.A. Raduta, Phys. Rev. C 76 (2007) 044306.
- [68] J. Suhonen, Nucl. Phys. A 700 (2002) 649.
- [69] P. Domin, S. Kovalenko, F. Simkovic, and S.V. Semenov, Nucl. Phys. A 753 (2005) 337.
- [70] S.K.L. Sjuue et al., Phys. Rev. C 78 (2008) 064317.